
JOSENet: A JOINT STREAM EMBEDDING NETWORK FOR VIOLENCE DETECTION IN SURVEILLANCE VIDEOS

Pietro Nardelli and Danilo Comminiello

Dept. of Information Engineering, Electronics and Telecommunications (DIET)
Sapienza University of Rome
Via Eudossiana 18 - 00184 Rome, Italy

ABSTRACT

Due to the ever-increasing availability of video surveillance cameras and the growing need for crime prevention, the violence detection task is attracting greater attention from the research community. With respect to other action recognition tasks, violence detection in surveillance videos shows additional issues, such as the presence of a significant variety of real fight scenes. Unfortunately, available datasets seem to be very small compared with other action recognition datasets. Moreover, in surveillance applications, people in the scenes always differ for each video and the background of the footage differs for each camera. Also, violent actions in real-life surveillance videos must be detected quickly to prevent unwanted consequences, thus models would definitely benefit from a reduction in memory usage and computational costs. Such problems make classical action recognition methods difficult to be adopted. To tackle all these issues, we introduce JOSENet, a novel self-supervised framework that provides outstanding performance for violence detection in surveillance videos. The proposed model receives two spatiotemporal video streams, i.e., RGB frames and optical flows, and involves a new regularized self-supervised learning approach for videos. JOSENet provides improved performance compared to self-supervised state-of-the-art methods, while requiring one-fourth of the number of frames per video segment and a reduced frame rate. The source code and the instructions to reproduce our experiments are available at github.com/ispamm/JOSENet.

Keywords Representation Learning · Self-Supervised Learning · Violence Detection · Action Recognition

1 Introduction

Violence detection is one of the most important and challenging sub-tasks of human action recognition [1]. Many violent events, like fighting, might arise from different situations and places (e.g., burglary, hate crimes, etc.) and it is rather difficult to detect them in an early stage to guarantee security [2]. Very few tools are available to detect and prevent violent actions. One of the most popular measures to increase public security is to adopt Closed-Circuit Television (CCTV) video surveillance systems. However, CCTVs still require an enormous manual inspection, which is often affected by human fatigue that may jeopardize quick decisions and crime avoidance [3, 4]. A significant alternative solution to raise the level of public safety is represented by the development of deep learning methods for the automatic detection of violent actions [4–7]. However, detecting violent scenes in surveillance videos entails several challenges, such as actors and backgrounds that may significantly differ among different videos, different lengths, or resource limitations due to real-time surveillance. Moreover, it is not easy to find available labeled datasets to effectively perform detection in a supervised fashion.

To address the above issues for the violence detection task, this work aims at introducing JOSENet, a novel joint stream embedding architecture involving a new efficient multimodal video stream network and a new self-supervised learning paradigm for video streams. In particular, the flow-gated network (FGN) [8] receives two video streams, a spatial RGB flow and a temporal optical flow, as shown in Fig. 1 (top). The proposed method adopts a very small number of frames per segment and a low frame rate with respect to state-of-the-art solutions in order to optimize the benefit-cost ratio from a production point of view. This cost reduction may lead, however, to an unwanted side-effect that can significantly affect performance accuracy. In order to compensate for such a performance decrease while

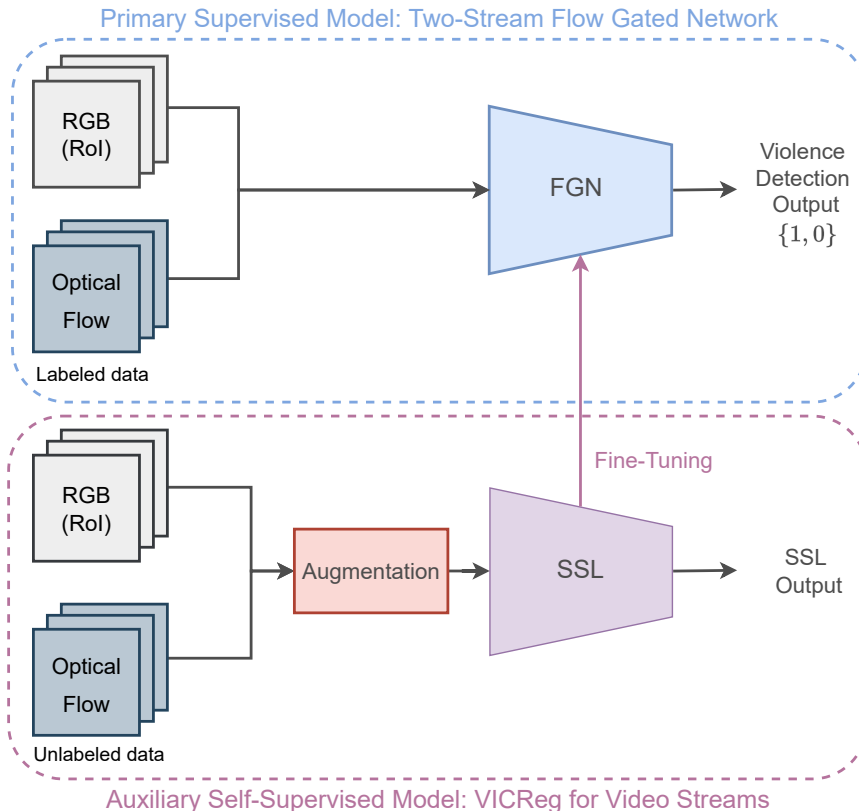


Figure 1: The proposed JOSENet framework. The primary target model (top) is tackled by using a novel efficient Flow Gated Network (FGN) which produces binary classification (1 if violence is detected, 0 otherwise) given optical flow and RGB segments. The FGN is pretrained by using a novel two-stream SSL method (bottom) that aims to solve an auxiliary task with unlabeled input data.

still reducing any overfitting, we initialize the network with pretrained weights by involving self-supervised learning (SSL) approaches, which produce useful representations without relying on inputs annotated by humans, as shown in Fig. 1 (bottom). In particular, besides testing many different state-of-the-art SSL methods suitable for JOSENet, we propose a novel SSL algorithm specifically designed for video streams and based on the variance-invariance-covariance regularization (VICReg) [9]. To the best of our knowledge, this is the first time a VICReg-like approach has been developed for a video stream architecture. The proposed SSL approach exploits the VICReg capabilities, thus, unlike other methods, it scales well with the dimension of the data, does not demand large memory, and prevents any collapse issue. The use of an SSL method makes JOSENet also robust to any lack of labeled data, which is often the case in real-life surveillance videos, and can improve the generalization capability of the model [10].

We prove the effectiveness of the proposed JOSENet framework over the most popular datasets of violence detection under several conditions, highlighting the advantages and drawbacks of our method. Results show that the proposed JOSENet model is able to efficiently reduce both the number of frames per video and the frame rate while outperforming existing SSL solutions.

2 Related work

Violence Detection. In the last years, the analysis of violent actions has become tractable thanks to deep neural networks. An early work employed a VGG16 for optical flows [11]. A modified Xception CNN is used in [1] together with a Bi-LSTM to learn the long-term dependency. Investigation on the use of bidirectional temporal encodings can be found in [12]. Besides introducing the CCTV-Fight dataset, 2D CNN VGG16 architectures were proposed in [2]. A framework with localization and recognition branches was proposed in [3]. Alternative approaches are based on the 3D skeleton point clouds, e.g., extracted from videos via a pose detection module [13–15]. In [6], several pretraining strategies were explored. Efficient spatio-temporal architectures were proposed in [5, 16].

Self-Supervised Learning. Self-supervised learning (SSL) aims at learning representations from unlabeled data, and building generalized models. The first SSL approaches were proposed for spatial context prediction [17] and Jigsaw puzzle solution [18]. The contrastive learning (CL) approach [19] discriminates between a set of augmented labels. The contrastive predictive coding [20] extracts useful representations from high-dimensional data. In [21], CL was applied to human activity recognition. While CL obtained competitive performance with respect to supervised representation [22, 23], it does not scale well with the dimension of the data, and it tends to require large memory demands. Regularized methods solve these problems [24, 25]. In particular, the Barlow Twins method [26] naturally avoids collapse by the measure of cross-correlation matrix between the two outputs of a Siamese neural network. Inspired by [26], the Variance-Invariance-Covariance Regularization (VICReg) [9] has been proposed for multimodal data, showing good scaling ability and limited memory demand. A new variant of VICReg for video streams is proposed for JOSENet.

Self-Supervised Learning for Video. Several SSL techniques were specifically proposed for video streams, starting from [27–29]. One of the first works acting on a two-stream architecture was presented in [30]. Spatiotemporal 3D CNNs were introduced in SSL by [31]. In [32], a task was defined to predict numerical labels. A method based on contrastive predictive coding for video representation learning was developed in [33]. Dense predictive coding was proposed for learning spatiotemporal video embeddings [34]. Differently, CoCLR [35] exploits complementary data (i.e., optical flow) as additional positive samples in a new co-training regime. The pretext-contrastive learning (PCL) [36] is a joint optimization framework for both CT and pretext tasks. The only work that uses SSL for the violence detection task introduces an iterative learning framework based on two experts feeding data to each other where the SSL expert is a C3D network [37]. The classification network involved in the proposed JOSENet framework is an advanced version of the C3D. Also, in [38], an SSL approach is adopted to pretrain a module for selecting informative frames for abnormal action recognition. Our aim instead, is to obtain a better-performing network without using additional modules that could slow down the inference speed, which is critical for violence detection.

3 Proposed method

The proposed JOSENet framework for violence detection is basically composed of two parts, as depicted in Fig. 1: a primary target model and an auxiliary SSL model. The target part is composed of the two-stream flow gated network, involving both spatial and temporal flows, which performs violent action detection using labeled data. The two-stream architecture guarantees significant performance. To reduce both memory and computational costs, we use a lightweight setting for the model in terms of the number of frames per video. The JOSENet framework benefits from an auxiliary model to avoid any loss of performance. This auxiliary network implements a novel SSL method receiving unlabeled data as input. The weights of the auxiliary model are optimized by minimizing the VICReg loss, and subsequently employed in the pretraining of the primary supervised model. Following the pretraining phase, a fine-tuning strategy is utilized to refine and tailor the pretrained weights to the specific requirements of the primary task. The auxiliary SSL network allows JOSENet to achieve the best trade-off between performance and employed resources. In the following, we focus in detail on the two models of the proposed framework.

3.1 Primary Model: An Efficient Two-Stream Flow Gated Network

The primary target model is based on a two-stream flow gated network (FGN). The choice of a two-stream architecture is motivated by the benefits brought by multimodal video architectures and by the excellent performance that the FGN achieved on the RWF-2000 dataset [8]. This network consists of three modules: a spatial block, a temporal block, and a merging block.

Spatial Block. The spatial RGB module receives as input consecutive frames that are cropped to extract the region of interest (ROI). The ROI aims to reduce the amount of input video data, making the network focus only on the area with larger motion intensity. The computation of the ROI involves normalization and a subtraction of the mean of each optical flow frame for denoising purposes. Given the normalized and denoised optical flow frame S_i , the magnitude can be computed as $(S_{i,x}^2 + S_{i,y}^2)^{\frac{1}{2}}$ where $S_{i,j}$ represents the j -th component of the i -th frame. The sum of the magnitudes of each frame produces a 224×224 motion intensity map, on which the mean is computed and used as a threshold to additionally filter out the noise (i.e., zeroing out the motion intensity map values if less than this threshold). To obtain the center of the ROI based on the motion intensity map, a probability density function along the two dimensions x, y of the motion intensity map is used. Ten different candidates are selected to be the center of the ROI, and are extracted randomly from this probability density function. The final value of the center (c_x, c_y) is obtained by the average of these 10 points for better robustness. The ROI is extracted by a patch of size 112×112 from the RGB frames based on (c_x, c_y) , thus a cubic interpolation is applied to reconstruct N frames with size 224×224 . Once processed, the

output of the RGB block passes through a ReLU activation function. The resulting input dimension of the RGB block is $3 \times N \times 224 \times 224$, where the first dimension represents the RGB channels of the video segment.

Temporal Block. The temporal block receives as input the optical flow of the sequence of frames. The flow is computed by using the Gunnar Farneback’s algorithm, as in [8]. For each RGB segment (F_0, F_1, \dots, F_s) of N frames of size 224×224 , an optical flow frame is computed from each couple (F_{i-1}, F_i) . The resulting dimension of the flow block is $2 \times N \times 224 \times 224$. A sigmoid activation function at the end of this branch scales the output for the RGB embeddings.

Merging Block. The last FGN module defines the fusion strategy that manages both the RGB and the flow streams. In particular, the output of the RGB block and the flow block are multiplied together and processed by a temporal max pooling. This is a self-learned pooling strategy that utilizes the flow block as a gate, aiming to decide which information from the RGB block should be maintained or dropped. Finally, the fully-connected layers generate the output for that input.

Computational Enhancement. Since violence detection is a real-time application, it is necessary to reduce the computational cost as much as possible, thus finding more efficient ways to produce inference [3], while deploying the model with reduced memory usage and frame rate during inference. To maintain the cost as low as possible, it is necessary to first deal with the number of frames N in the input video segment while, at the same time, the network should be able to learn the correct features by using a correct window size T_{tf} (temporal footprint). The vanilla FGN [8] uses $N = 64$ frames with $N_{\text{fps}} = 12.8$ frames per second (FPS). Instead, to speed up the inference, we use $N = 16$ which is a common value for the most used action recognition architectures such as R(2+1)D [39], C3D [40], I3D [41] and P3D [42]. In action recognition, it is known that a very short window can lead to perfect recognition of most activities [43] while at the same time, the classification performance generally increases by using a very high frame rate. However, as pointed out in [44], action recognition methods do not always obtain their best performance at higher frame rates, but the best results are achieved by each method at different frame rates. In this way, we treat N_{fps} like a hyperparameter that we aim to reduce for practical reasons. Thus, we find that a value of $N_{\text{fps}} = 7.5$ is an optimal trade-off between computational cost and performances, obtaining as a result a temporal footprint of $T_{\text{tf}} = \frac{N}{N_{\text{fps}}} = 2.13\text{s}$. This choice can be considered appropriate for the broad category of violent actions. Further generalization performance can be found in Section 4.3.

Efficient Implementation. To reduce the segment length N we modify the $2 \times 2 \times 2$ max-pooling layers of the merging block into a $1 \times 2 \times 2$ (i.e., reducing by 1 the temporal dimension) so that the output dimension for that block is unchanged. In addition, to approximately halve the memory requirements while speeding up arithmetic, we use mixed-precision [45]. With the aim of reducing the internal covariance shift, a 3D batch-norm layer is applied after each activation function of all the blocks of our architecture, except for the fully connected (FC) layers. Lastly, to avoid overfitting, spatial dropout with $p = 0.2$ is applied after each batch normalization layer of the first two 3D convolutional blocks, in both RGB and optical flow blocks. The proposed model achieves a significant reduction of computational complexity compared to the original network in [8]. Specifically, our model required only 4.432G multiply-accumulate operations (MACs), whereas the original architecture demanded 33.106G MACs, indicating a **7-fold reduction in computational load**. In addition, through a 4x smaller segment size and a reduced temporal footprint, we are able to significantly **reduce the memory requirements by 75%** and achieve a **two-fold increase in signaling alarm speed in real-life scenarios**. This result highlights the potential of our framework for efficient and effective neural network design. One might view these findings as addressing a inefficiency rather than introducing a new algorithm — yet, this perspective does not diminish their significance.

3.2 Auxiliary Model: VICReg for Joint Video Stream Architectures

Self-Supervised Pretraining. The original FGN [8] does not involve any pretraining. In this work instead, we investigate the use of self-supervised pretraining as opposed to fine-tuning approaches 1) to compensate for the performance loss due to the resource limitation of the primary network, 2) to deal with unlabeled data typical of real-world surveillance video applications, and 3) to improve the generalization performance by avoiding a bias toward the source labels on the source task [10]. We implemented four different SSL techniques: odd-one-out (O3D) [28], arrow of time (AoT) [46], space-time cubic puzzle (STCP) [31], and VICReg [9]. Clearly, all the above SSL techniques are fairly adapted to our FGN.

Proposed VICReg for JOSENet. In our framework, we focus on the variance-invariance-covariance regularization (VICReg) [9], an SSL method for joint embedding architectures that preserves the information content of the embeddings,

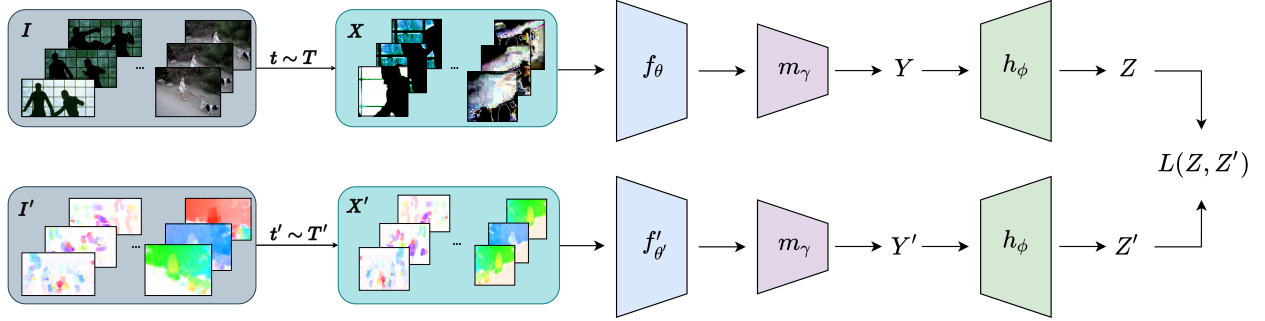


Figure 2: The proposed VICReg solution for the JOSENet framework. I and I' are respectively a batch of RGB and flow segments that are transformed through data augmentation into two different views X and X' . In particular, a strong random cropping strategy and some other augmentation techniques are applied to RGB frames while the flow frames are only flipped horizontally. The RGB branch is represented by f_θ , the optical flow branch is $f'_{\theta'}$, m_γ is the merging block without the temporal max pooling and finally, the h_ϕ is the expander as in the VICReg original implementation. The VICReg loss function $L(Z, Z')$ is computed on the embeddings Z and Z' .

while not demanding large memory requirements, contrastive samples nor memory banks, unlike what happens in contrastive methods [47]. To the best of our knowledge, for the first time VICReg is applied to video streams. The proposed VICReg solution for JOSENet relies on the joint information of the augmented RGB and flow batches and it is depicted in Fig. 2.

Let us consider an RGB batch I and an optical flow batch I' both related to the same input segment. Two augmented views of these batch X and X' can be produced by using random transformations t and t' sampled from a distribution T . The augmented batches are fed into two different encoders f_θ and $f'_{\theta'}$. The two branches do not have the same architectures and do not share the same weights. The output of these branches is fed as input into two Siamese merging blocks m_γ that have the same architecture as the merging block but without the temporal max pooling. Indeed, the removal of this pooling seems to be beneficial thanks to the increase of the expander input dimensionality. The output representations Y and Y' are fed as input into two Siamese expanders h_ϕ which produces batches of embeddings $Z = h_\phi(Y)$ and $Z' = h_\phi(Y')$ of n vectors of dimension d . By utilizing the Siamese merging block during the self-supervised phase, we are able to generate representations of the input data by leveraging a significant portion of the FGN architecture. As a result of this approach, we are able to obtain highly informative and useful feature representations of the input data, which can subsequently be utilized for the primary task. This particular solution would be infeasible with other SSL techniques and can be designed only by using a method that can handle multimodality, such as VICReg. Indeed, among the several configurations tested, we will demonstrate that this is the best setup for pretraining our two-stream FGN. We leverage the basic idea of VICReg to use a loss function with three different terms. The variance regularization term $v(Z)$ is computed along the batch dimension as the standard deviation of the embeddings and aims to prevent a complete collapse. The covariance regularization term $c(Z)$ encourages the network to decorrelate the dimensions of the embeddings so that similar information is not encoded. This kind of decorrelation at the embedding level leads to a decorrelation at the representation level as well. Our approach entails to diminish the disparities between the two data modalities through the minimization of the invariance term $s(Z, Z')$ which is the mean-squared Euclidean distance between each pair of embedding vectors. The overall loss function $L(Z, Z')$ is a weighted average of these terms:

$$L(Z, Z') = \lambda s(Z, Z') + \mu [v(Z) + v(Z')] + \nu [c(Z) + c(Z')] \quad (1)$$

where λ, μ and ν are hyperparameters (specifically, $\lambda = \mu = 25$ and $\nu = 1$ works best in most of the contexts). Since VICReg is an information maximization method, it does not require the use of techniques generally used in contrastive methods. Moreover, although it was proposed for a Siamese network [9], one of its greatest advantages is that the two branches could also not share the same parameters, architectures, and more importantly input modality.

Configuration. In [9], the input size of the expanders h_ϕ is set to 2048. In our case, using a merging block m_γ with an unchanged structure would produce an input of size 128. Since it is paramount to include most of the two-stream architecture without reducing too much the expander dimensionality, we remove the temporal max-pooling in the merging block. In this way, the expander input dimensionality grows from 128 to 1024, finding a good trade-off between the two constraints. Thus, the output representations Y and Y' have dimension 1024 and are fed as input into the two

Siamese expanders h_ϕ . The expanders have the same structure as the original method: 3 FC layers of size 8192, where the first two layers utilize batch normalization and ReLU.

4 Experimental Results

4.1 Experimental Settings

Datasets. To train and validate the model for supervised learning we use the RWF-2000 dataset [8], involving 2,000 heterogeneous videos, 5 seconds long, and captured at $N_{fps} = 30$ FPS by real-world surveillance cameras. In line with the existing literature, we also use HMDB51 [48] (51 classes spread over 6,766 clips) and UCF101 [49] (nearly twice the size of HMDB51) datasets. Although a larger dataset can be beneficial in most cases, SSL techniques generally outperform transfer learning when the amount of pretraining is small [10]. Moreover, since a strong domain similarity can be very useful [10], we use the UCF-Crime [50] as an additional dataset. We maintain the default train-test split in all the datasets used in both target and auxiliary tasks.

Preprocessing Methods. We use the same frame resolution as in [8] (224×224) with each video segment generated with $N_{fps} = 7.5$ FPS in a sliding window manner [43].

Data Augmentation. In the target task, we apply color jitter to RGB frames and random flip to both RGB and flow frames. On the other hand, for each auxiliary task, we use different kinds of augmentations. For the proposed VICReg, differently from [9], we use a stronger random cropping strategy in the RGB augmentation pipeline, by imposing a scaling factor within the range $[0.08, 0.1]$, which is confirmed to be more efficient from our tests. We call this augmentation the “zoom crop” strategy. For what concerns the flow segments, a simple horizontal flip (with 50% probability) is applied. A visualization of the VICReg video input for the JOSENet framework can be seen in Fig. 2.

Metrics. Similarly to [4], we evaluate the performance by the following metrics: the accuracy, F1-score, true negative rate (TNR), true positive rate (TPR), and the area under the curve (AUC) to understand the model diagnostic capability in identifying violent videos. We enhance the model’s performance by optimizing the accuracy, the primary evaluation metric in the majority of violence detection methodologies. However, we recognize that the application of violence detection carries ethical responsibilities. For this reason, we prioritized metrics (i.e., TNR) that reduce the false positive rate which could cause innocent individuals to be wrongly accused or flagged as potential threats.

4.2 Experimental Results Without Pretraining

The first experiments aim to find the best baseline model without self-supervised pretraining. We first tackle the hyperparameter tuning from which we found our best parameters for the network. More specifically, we train the network on 32 batches for a total of 30 epochs together with an early stopping procedure with a patience of 15 epochs. The number of frames for each segment is $N = 16$, sampled at $N_{fps} = 7.5$ FPS. We use a $p = 0.2$ dropout probability for the classification block. A binary cross-entropy loss is employed with a stochastic gradient descent (SGD) optimizer (momentum 0.9 and $1e-6$ weight decay), as it is a state-of-the-art choice for violent detection [8]. A cosine annealing scheduler is implemented, which starts from the initial learning rate value of 0.01, and decreases for 30 epochs to reach a minimum of 0.001. With these settings, we obtain 84.25% accuracy. To avoid overfitting at this stage, we add spatial dropout with a probability of 0.2. In this case, we obtain 85.87% accuracy, thus we increase it by +1.62%, F1-Score 85.87%, 85.5% TNR, 86.25% TPR, and 0.924 AUC. We use this model as a “baseline” for comparisons.

4.3 Experimental Results with Self-Supervised Learning

Now we evaluate the target task using the embeddings obtained with SSL pretraining. In particular, for each technique, we pretrain on three different datasets: HMDB51, UCF101, and UCF-Crime. During pretraining we use the same hyperparameters of the target task with the difference in weight decay value of $1e-6$ while epochs and batch size vary based on the technique used. In each trial, we maintain the maximum number of iterations of the cosine annealing scheduler equal to the number of epochs. While for VICReg we use the custom loss described by eq. 1, in all the other techniques a cross-entropy loss is applied. A fine-tuning strategy is applied by training the primary model on the target task.

JOSENet with non-regularized SSL approaches. Results for JOSENet with non-regularized SSL methods are shown in Table 1. As expected, the O3D technique does not provide useful embeddings for the target task. In fact, the results are all worse than the baseline model by a wide margin. It is useful to note that the results are better in

Table 1: Results obtained by pretraining our FGN using the non-regularized SSL methods and fine-tuning it on the target task. Each SSL method is tested with a different dataset for pretraining.

SSL	Dataset	Accuracy [%]	F1 [%]	TNR [%]	TPR [%]	AUC
O3D [28]	HMDB51	82.62	82.62	84	81.25	0.897
O3D [28]	UCF101	82.75	82.74	82.25	83.25	0.888
O3D [28]	UCF-Crime	83.37	83.37	83.75	83	0.901
AoT [46]	HMDB51	84.75	84.74	86.25	83.25	0.911
AoT [46]	UCF101	84.5	84.49	82.75	86.25	0.911
AoT [46]	UCF-Crime	84	83.97	80	88	0.900
STCP [31]	HMDB51	-	-	-	-	-
STCP [31]	UCF101	86.25	86.25	85.25	87.25	0.913
STCP [31]	UCF-Crime	85.25	85.23	88.75	81.75	0.912

Table 2: Results obtained by our proposed VICReg method on a random 15% subset of the datasets UCF101 (R-UCF101) and UCF-Crime (R-UCF-Crime). In particular, R-UCF-Crime surpasses by a wide margin R-UCF101 on TPR and more importantly on F1-score. The final results obtained with a pretraining on the entire UCF-Crime dataset are shown in the last row.

Dataset	Accuracy [%]	F1 [%]	TNR [%]	TPR [%]	AUC
HMDB51	85.37	85.37	84	86.75	0.924
R-UCF101	86.37	86.37	85.75	87	0.922
R-UCF-Crime	86.75	86.74	84.5	89	0.918
UCF-Crime	86.5	86.5	88	85	0.924

UCF-Crime, while HMDB51 produces the worst pretraining weights. For what concerns the Arrow of Time (AoT) method, the results are unsatisfactory, probably because this technique (like the O3D one) is strongly dependent on the architecture chosen (in both cases they rely on 2D CNNs). It is interesting to see that the HMDB51 and UCF101 obtain similar results while UCF-Crime produces the worst performance. This may due to a trivial learning problem due to low-level cues. This is also confirmed by the high accuracy obtained on the auxiliary task itself. For STCP some improvements are achieved by using the UCF101 dataset. It is important to point out that we obtained a slight improvement compared to the baseline model and higher results compared to the other SSL pretraining. Differently from the previous methods, the STCP is built to be used on 3D CNNs, confirming that the architecture similarity plays an important role in the choice of the correct non-regularized SSL technique used.

JOSENet with Pretraining Dataset Selection for VICReg. We focus the attention on an approach without shared weights by pretraining simultaneously both RGB and optical flow branches. We assume that the best configuration involves a zoom crop strategy without considering the temporal max-pooling in the merging block. To validate this hypothesis and understand the best dataset for pretraining we test on the remaining two datasets: UCF101 and UCF-Crime. To provide a fair comparison between HMDB51 and the remaining ones, while maintaining a feasible training time (i.e., each pretraining on the HMDB51 dataset lasts around 12 hours), in this phase, we pretrain on a subset of UCF101 and UCF-Crime, denoted as R-UCF101 and R-UCF-Crime respectively. The “R” signifies “Reduced”, indicating that we randomly sample 15% of each dataset, using 16 batches for training. The results are shown in Table 2. As we can see, VICReg pretrained on R-UCF101 outperforms the best model obtained so far. Compared to the baseline, we show an increase in accuracy (+0.5%), F1-score (+0.5%), TNR (+0.25%), and TPR (+0.75%). Similarly, the model pretrained on R-UCF-Crime and tested on the target task shows a huge increase in performance in terms of F1-score (+0.87 %) and TPR (+2.75 %). This result underscores the importance of the quality of the dataset for the auxiliary task. Moreover, as expected, the dataset domain similarity between auxiliary and target tasks seems to be beneficial, resulting in an important factor to be considered when choosing the pretraining dataset.

Final Results for JOSENet. To obtain our best performances and to further validate our solution, we train our best configuration on the entire UCF-Crime dataset using an NVIDIA Tesla V100S GPU with 32GB GPU RAM and CPU Intel Xeon Gold 6226R CPU @ 2.90GHz with 15 cores, thus increasing the batch size from 16 to 64. In this case, we directly drop the merging block pretrained weights. This behavior suggests that the merging block weights (like the expander ones) are very important only during the pretraining phase. In other words, the merging block in VICReg helps the RGB and flow branches to learn the correct features but, with the increase of the batch size, the role of the merging block weights remains fundamental in VICReg while losing its relevance in the target task. The final results shown in Table 2 meet our expectations. We reach an **accuracy and F1-score of 86.5% (+0.63%)** which is a solid improvement compared to the baseline model. The confusion matrix shown in Fig. 3 (left) indicates that the model

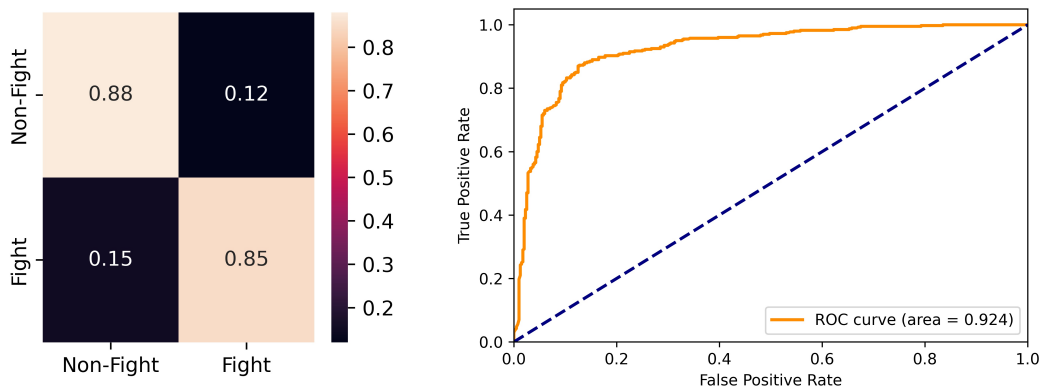


Figure 3: Normalized confusion matrix (left) and ROC curve (right) obtained by evaluating our best model on the RWF-2000 validation set by pretraining via our VICReg proposed method with 64 batch size on the entire UCF-Crime dataset. The rows and columns of the confusion matrix represent respectively the predicted and target labels.

Table 3: The evolution of the results of our JOSENet framework. The first row shows the results of the baseline model. The final results are shown in the last row.

Dataset	Accuracy [%]	F1 [%]	TNR [%]	TPR [%]	AUC
No-pretraining	85.87	85.87	85.5	86.25	0.924
R-UCF-Crime	86.75	86.74	84.5	89	0.918
UCF-Crime	86.5	86.5	88	85	0.924

reaches **88% (+2.5%) in TNR** and **85% (-1.25%) in TPR**. While a decrease in the TPR rate is acceptable, the increase in TNR is well received. In fact, from an application point of view, the TNR is an important metric that avoids stressing out the user with excessive false positives, given that the number of non-violence samples would be greater than the violent ones in a real case scenario. Furthermore, by reducing false positives, we can mitigate the risk of wrongful actions that could be taken against individuals who are mistakenly identified as violent. For the sake of completeness, we show also the ROC curve in Fig. 3 (right). The **AUC reaches a value of 0.924** which is similar to the baseline model, demonstrating a good capability to distinguish between classes. Although JOSENet performs slightly worse than the state of the art for RWF-2000 [8], it clearly represents a more efficient and faster solution thanks to a four-time smaller segment length (16 instead of 64) and a smaller FPS required (7.5 instead of 12.8). This proves that the proposed framework features an excellent compromise between performance and efficiency.

We outlined the JOSENet performance evolution in Table 3. The first model does not involve any pretraining: the primary task has been addressed directly by the FGN trained on the RWF-2000 training set. Then, we implemented several non-regularized SSL strategies that produced slightly improved results, compared to the baseline. For this reason, we used VICReg as an auxiliary SSL model in our JOSENet framework. With the aim of selecting the best pretraining dataset for JOSENet we have seen that R-UCF-Crime obtained the higher results (see the second row of Table 3). Finally, we pretrained the auxiliary SSL VICReg model on the entire UCF-Crime, reaching the final results for JOSENet, shown in the last row of Table 3.

SSL State-of-the-Art Comparison. In this section, we compare JOSENet with previous SOTA self-supervised approaches: InfoNCE [20], UberNCE [35] and CoCLR [35]. We decide to take as reference the results obtained on R-UCF-101 with JOSENet. For a fair comparison, we pretrain on the same dataset either RGB or flow blocks using the SOTA methods by scaling down accordingly some of their hyperparameters. Then, as usual, the obtained weights are used as pretraining for the target task. The results are shown in Table 4. We can observe that InfoNCE surpasses both the accuracy and F1-score performance of JOSENet and all the other methods when only the RGB or the flow blocks is pretrained. However, the AUC results show that UberNCE is still a valid alternative to the instance-based SSL in such a situation. As expected, when two pre-trained branches are used, CoCLR has better AUC performance compared to all the other SOTA methods thanks mainly to the co-training scheme. Nevertheless, a huge drop in performance happens in the SOTA methods compared to JOSENet, which obtains the best results on this setting: +1.28% accuracy and F1-score, with +0.011 AUC from the second best method. These results can be explained by the fact that all the

Table 4: Representations from InfoNCE, UberNCE, CoCLR and JOSENet are evaluated on the target task, with a pretraining obtained on a R-UCF-101. The \times indicates the random initialization of the branch during target training. In the last rows, we simultaneously initialize both the RGB and flow blocks of the FGN model.

Method	RGB	Flow	Accuracy [%]	F1 [%]	TNR [%]	TPR [%]	AUC
InfoNCE [20]	✓	✗	85.12	85.12	84	86	0.906
UberNCE [35]	✓	✗	84.5	84.5	77	92	0.911
CoCLR [35]	✓	✗	84.25	84.25	84	84	90.86
JOSENet (ours)	✓	✗	84.62	84.62	85.75	83.5	0.917
InfoNCE [20]	✗	✓	85.12	85.12	87	83	0.907
UberNCE [35]	✗	✓	84	83.99	86	82	0.905
CoCLR [35]	✗	✓	84.25	84.25	84	84	0.908
JOSENet (ours)	✗	✓	84.49	84.49	82.75	86.75	0.900
InfoNCE [20]	✓	✓	83.62	83.59	89	79	0.897
UberNCE [35]	✓	✓	83.87	83.80	91	77	0.895
CoCLR [35]	✓	✓	83.5	83.44	90	78	0.898
JOSENet (ours)	✓	✓	86.4	86.4	85.75	87	0.922

Table 5: Action recognition results of our FGN pretrained with VICReg on UCF-Crime. The last two columns represent respectively the Top-1 and Top-5 accuracy computed on fold 1 for both datasets.

Dataset	VICReg Pretraining	Top-1 [%]	Top-5 [%]
HMDB51	✗	20	49.03
HMDB51	✓	24.62	55.03
UCF101	✗	43.18	70.12
UCF101	✓	48.1	73.24

SOTA methods do not take into consideration the merging block of the FGN while JOSENet is able to exploit that part of the architecture during pretraining, thus producing better embeddings for the target task.

Generalizing JOSENet to Action Recognition Tasks. As an additional test, we use our JOSENet framework pretrained with VICReg on the UCF-Crime dataset as a starting point for the action recognition task. In particular, we fine-tune the FGN on two different benchmark datasets for action recognition: HMDB51 and UCF101. In order to avoid any overfitting of the network on dynamic actions, the only modification that we apply is the removal of the RoI extraction for the RGB frames. The entire training procedure and the architecture remain unchanged compared to the one described in the previous sections. The results in Table 5 show that our pretraining based on the VICReg seems to be effective also for a more generic action recognition task. Indeed, in both the datasets we obtain a boost in performances of about 3-6% of accuracy. We want to highlight that our architecture trained from scratch surpasses by 1-3% Top-1 accuracy of the Resnet3D-18 [51], which requires a huge computational power (33.3M parameters) compared to the FGN network (272,690 parameters). Thus, we strongly believe our JOSENet framework could obtain near state-of-the-art performance by exploiting a pretraining obtained on a larger dataset (i.e., Kinetics).

5 Ablation Studies

Siamese Architecture. With the aim to understand if a simpler Siamese architecture can be sufficient for good pretraining, we pretrain either RGB or flow branches with shared weights. In both cases, we pretrain the branches on HMDB51. During the target task training, the non-pretrained block is randomly initialized. As an additional experiment, to avoid this random initialization, the resulting pretrained blocks are used simultaneously in the target task. The results are shown in Table 6. All these approaches seem to be inefficient, confirming that in order to improve the embeddings of both RGB and flow branches, JOSENet needs to use the complementary information provided by both RGB and flow views during the pretraining phase.

Augmentation Strategies. The results on different architecture and augmentation strategies are shown in Table 7. We first pretrain our model by using the zoom crop strategy. At the same time, we try to avoid an excessive reduction in the dimensionality of the expander input by removing the temporal max-pooling in the merging block. While the results on the accuracy are slightly lower than our baseline, we obtain an increase in TPR by +0.50% and a slight increase in AUC suggesting a feasible model configuration. To find a confirmation of this approach, using the zoom crop strategy, we apply the temporal pooling in the merging block, obtaining on the target task a very low value for most of the evaluation

Table 6: Results of the target task achieved through pretraining with the VICReg method on HMDB51 dataset, utilizing two Siamese branches, either RGB or flow. The \times indicates the random initialization of the branch during target training. In the last row, we used simultaneously the previously pretrained Siamese models on the target task.

RGB	Flow	Accuracy	F1 [%]	TNR [%]	TPR [%]	AUC
✓	✗	84.62	84.62	85.75	83.5	0.917
✗	✓	84.5	84.49	82.07	87.03	0.918
✓	✓	84.37	84.37	82.75	86.75	0.900

Table 7: Results obtained on the target task by pretraining the VICReg on HMDB51 using different configurations. In particular, we test our model by including or removing the zoom crop (ZC) augmentation strategy and/or the temporal max-pooling (TMP) in the merging block.

ZC	TMP	Accuracy [%]	F1 [%]	TNR [%]	TPR [%]	AUC
✓	✗	85.37	85.37	84.01	86.75	0.924
✓	✓	82.5	82.49	84.75	80.25	0.8927
✗	✗	85.25	85.22	90.15	81.57	0.9159

metrics used. This test shows that some issues occur when there is a very small bottleneck between the encoder and the expander. In fact, the input expander dimensionality is reduced from 1024 to 128. Successively, the network is pretrained with the random crop [9] while avoiding the temporal pooling in the merging block. The results are not optimal and suggest that zoom crop augmentation is crucial for the network to extrapolate the most useful features.

6 Conclusion and future work

In this work, we introduced JOSENet, a novel regularized SSL framework involving a modified VICReg for a two-stream video architecture. The proposed framework is able to tackle effectively the violence detection task, a challenging research topic in computer vision. The proposed JOSENet framework has proven to achieve high performance for violence detection, while maintaining solid generalization capability, as it is able also to detect non-violent actions. These results are the basis for product stability from an application deployment perspective. Furthermore, our experiments showcase that JOSENet outperforms state-of-the-art SSL methods in the domain of violence detection, underscoring its superior performance in this task. Lastly, we assess the robustness and generality of the framework by deploying it in generic action recognition tasks. In the future, it would be interesting to focus on possible limitations, e.g., avoiding any possible bias in unfair prediction, reducing the risk of false negatives, assessing the robustness against real-world issues on data (e.g., occlusions, light conditions), and improving the efficiency of the optical flow branch.

Data Availability

All the data used in this paper are publicly available. The UCF-Crime dataset [50] is composed of 128 hours of real-world surveillance videos and it is available at <https://www.crcv.ucf.edu/data/UCF101.php>. The RWF-2000 dataset [8], available at <https://github.com/mchengny/RWF2000-Video-Database-for-Violence-Detection>, is made of 2000 videos, 5 seconds long, and captured at 30 FPS by real-world surveillance cameras. The HMDB51 dataset [48] contains 51 classes spread over 6,766 clips and it is available at <https://serre-lab.clps.brown.edu/resource/hmdb-a-large-human-motion-database/>. A larger dataset called UCF101 [49] is available at <https://www.crcv.ucf.edu/data/UCF101.php>.

References

- [1] Seymanur Akti, Gozde Ayse Tataroglu, and Hazım Kemal Ekenel. Vision-based Fight Detection from Surveillance Cameras. *2019 Ninth International Conference on Image Processing Theory, Tools and Applications (IPTA)*, pages 1–6, November 2019. arXiv: 2002.04355.
- [2] Mauricio Perez, Alex C. Kot, and Anderson Rocha. Detection of Real-world Fights in Surveillance Videos. In *ICASSP 2019 - 2019 IEEE International Conference on Acoustics, Speech and Signal Processing (ICASSP)*, pages 2662–2666, Brighton, United Kingdom, May 2019. IEEE.

- [3] Qichao Xu, John See, and Weiyao Lin. Localization Guided Fight Action Detection in Surveillance Videos. In *2019 IEEE International Conference on Multimedia and Expo (ICME)*, pages 568–573, Shanghai, China, July 2019. IEEE.
- [4] Paolo Sernani, Nicola Falcionelli, Selene Tomassini, Paolo Contardo, and Aldo Franco Dragoni. Deep learning for automatic violence detection: Tests on the AIRTLab dataset. *IEEE Access*, pages 1–1, 2021.
- [5] Zahidul Islam, Mohammad Rukonuzzaman, Raiyan Ahmed, Md Hasanul Kabir, and Moshir Farazi. Efficient two-stream network for violence detection using separable convolutional LSTM. In *2021 International Joint Conference on Neural Networks (IJCNN)*, pages 1–8, July 2021. arXiv:2102.10590 [cs].
- [6] Shakil Ahmed Sumon, Raihan Goni, Niyaz Bin Hashem, Tanzil Shahria, and Rashedur M. Rahman. Violence detection by pretrained modules with different deep learning approaches. *Vietnam Journal of Computer Science*, 07(01):19–40, February 2020.
- [7] Fath U Min Ullah, Mohammad S. Obaidat, Khan Muhammad, Amin Ullah, Sung Wook Baik, Fabio Cuzzolin, Joel J. P. C. Rodrigues, and Victor Hugo C Albuquerque. An intelligent system for complex violence pattern analysis and detection. *International Journal of Intelligent Systems*, page int.22537, July 2021.
- [8] Ming Cheng, Kunjing Cai, and Ming Li. RWF-2000: An Open Large Scale Video Database for Violence Detection. In *2020 25th International Conference on Pattern Recognition (ICPR)*, pages 4183–4190, Milan, Italy, January 2021. IEEE.
- [9] Adrien Bardes, Jean Ponce, and Yann LeCun. Vicreg: Variance-invariance-covariance regularization for self-supervised learning, 2021.
- [10] Xingyi Yang, Xuehai He, Yuxiao Liang, Yue Yang, Shanghang Zhang, and Pengtao Xie. Transfer Learning or Self-supervised Learning? A Tale of Two Pretraining Paradigms. *arXiv:2007.04234 [cs, stat]*, June 2020. arXiv: 2007.04234.
- [11] Subham Mukherjee, Rajkumar Saini, Pradeep Kumar, Partha Pratim Roy, Debi Prosad Dogra, and Byung-Gyu Kim. Fight Detection in Hockey Videos using Deep Network. *Journal of Multimedia Information System*, 4(4):225–232, December 2017.
- [12] Alex Hanson, Koutilya PNVN, Sanjukta Krishnagopal, and Larry Davis. Bidirectional convolutional lstm for the detection of violence in videos. In Laura Leal-Taixé and Stefan Roth, editors, *Computer Vision – ECCV 2018 Workshops*, pages 280–295, Cham, 2019. Springer International Publishing.
- [13] Yukun Su, Guosheng Lin, Jinhui Zhu, and Qingyao Wu. Human interaction learning on 3D skeleton point clouds for video violence recognition. In Andrea Vedaldi, Horst Bischof, Thomas Brox, and Jan-Michael Frahm, editors, *Computer Vision – ECCV 2020*, volume 12349, pages 74–90. Springer International Publishing, Cham, 2020. Series Title: Lecture Notes in Computer Science.
- [14] Guillermo Garcia-Cobo and Juan C. SanMiguel. Human skeletons and change detection for efficient violence detection in surveillance videos. *Computer Vision and Image Understanding*, 233:103739, 2023.
- [15] Ryo Hachiuma, Fumiaki Sato, and Taiki Sekii. Unified Keypoint-Based Action Recognition Framework via Structured Keypoint Pooling. In *2023 IEEE/CVF Conference on Computer Vision and Pattern Recognition (CVPR)*, pages 22962–22971, Vancouver, BC, Canada, June 2023. IEEE.
- [16] Min-Seok Kang, Rae-Hong Park, and Hyung-Min Park. Efficient spatio-temporal modeling methods for real-time violence recognition. *IEEE Access*, 9:76270–76285, 2021.
- [17] Carl Doersch, Abhinav Gupta, and Alexei A. Efros. Unsupervised Visual Representation Learning by Context Prediction. *arXiv:1505.05192 [cs]*, January 2016. arXiv: 1505.05192.
- [18] Mehdi Noroozi and Paolo Favaro. Unsupervised Learning of Visual Representations by Solving Jigsaw Puzzles. *arXiv:1603.09246 [cs]*, August 2017. arXiv: 1603.09246.
- [19] Alexey Dosovitskiy, Philipp Fischer, Jost Tobias Springenberg, Martin Riedmiller, and Thomas Brox. Discriminative Unsupervised Feature Learning with Exemplar Convolutional Neural Networks. *arXiv:1406.6909 [cs]*, June 2015. arXiv: 1406.6909.
- [20] Aaron van den Oord, Yazhe Li, and Oriol Vinyals. Representation Learning with Contrastive Predictive Coding. *arXiv:1807.03748 [cs, stat]*, January 2019. arXiv: 1807.03748.
- [21] Harish Haresamudram, Irfan Essa, and Thomas Ploetz. Contrastive Predictive Coding for Human Activity Recognition. *arXiv:2012.05333 [cs]*, December 2020. arXiv: 2012.05333.
- [22] Ting Chen, Simon Kornblith, Mohammad Norouzi, and Geoffrey Hinton. A Simple Framework for Contrastive Learning of Visual Representations. *arXiv:2002.05709 [cs, stat]*, June 2020. arXiv: 2002.05709.

- [23] Kaiming He, Haoqi Fan, Yuxin Wu, Saining Xie, and Ross Girshick. Momentum Contrast for Unsupervised Visual Representation Learning. *arXiv:1911.05722 [cs]*, March 2020. arXiv: 1911.05722.
- [24] Jean-Bastien Grill, Florian Strub, Florent Alché, Corentin Tallec, Pierre H. Richemond, Elena Buchatskaya, Carl Doersch, Bernardo Avila Pires, Zhaohan Daniel Guo, Mohammad Gheshlaghi Azar, Bilal Piot, Koray Kavukcuoglu, Rémi Munos, and Michal Valko. Bootstrap your own latent: A new approach to self-supervised Learning. *arXiv:2006.07733 [cs, stat]*, September 2020. arXiv: 2006.07733.
- [25] Mathilde Caron, Ishan Misra, Julien Mairal, Priya Goyal, Piotr Bojanowski, and Armand Joulin. Unsupervised Learning of Visual Features by Contrasting Cluster Assignments. *arXiv:2006.09882 [cs]*, January 2021. arXiv: 2006.09882.
- [26] Jure Zbontar, Li Jing, Ishan Misra, Yann LeCun, and Stéphane Deny. Barlow Twins: Self-Supervised Learning via Redundancy Reduction. *arXiv:2103.03230 [cs, q-bio]*, June 2021. arXiv: 2103.03230.
- [27] Ishan Misra, C. Lawrence Zitnick, and Martial Hebert. Shuffle and Learn: Unsupervised Learning using Temporal Order Verification. *arXiv:1603.08561 [cs]*, July 2016. arXiv: 1603.08561.
- [28] Basura Fernando, Hakan Bilen, Efstratios Gavves, and Stephen Gould. Self-Supervised Video Representation Learning with Odd-One-Out Networks. In *2017 IEEE Conference on Computer Vision and Pattern Recognition (CVPR)*, pages 5729–5738, Honolulu, HI, July 2017. IEEE.
- [29] Hsin-Ying Lee, Jia-Bin Huang, Maneesh Singh, and Ming-Hsuan Yang. Unsupervised Representation Learning by Sorting Sequences. *arXiv:1708.01246 [cs]*, August 2017. arXiv: 1708.01246.
- [30] Ahmed Taha, Moustafa Meshry, Xitong Yang, Yi-Ting Chen, and Larry Davis. Two Stream Self-Supervised Learning for Action Recognition. *arXiv:1806.07383 [cs]*, June 2018. arXiv: 1806.07383.
- [31] Dahun Kim, Donghyeon Cho, and In So Kweon. Self-Supervised Video Representation Learning with Space-Time Cubic Puzzles. *Proceedings of the AAAI Conference on Artificial Intelligence*, 33:8545–8552, July 2019.
- [32] Jiangliu Wang, Jianbo Jiao, Linchao Bao, Shengfeng He, Yunhui Liu, and Wei Liu. Self-Supervised Spatio-Temporal Representation Learning for Videos by Predicting Motion and Appearance Statistics. In *2019 IEEE/CVF Conference on Computer Vision and Pattern Recognition (CVPR)*, pages 4001–4010, Long Beach, CA, USA, June 2019. IEEE.
- [33] Guillaume Lorre, Jaonary Rabarisoa, Astrid Orcesi, Samia Ainouz, and Stephane Canu. Temporal Contrastive Pretraining for Video Action Recognition. In *2020 IEEE Winter Conference on Applications of Computer Vision (WACV)*, pages 651–659, Snowmass Village, CO, USA, March 2020. IEEE.
- [34] Tengda Han, Weidi Xie, and Andrew Zisserman. Video Representation Learning by Dense Predictive Coding. In *2019 IEEE/CVF International Conference on Computer Vision Workshop (ICCVW)*, pages 1483–1492, Seoul, Korea (South), October 2019. IEEE.
- [35] Tengda Han, Weidi Xie, and Andrew Zisserman. Self-supervised co-training for video representation learning. In *Neurips*, 2020.
- [36] Li Tao, Xueting Wang, and Toshihiko Yamasaki. Pretext-Contrastive Learning: Toward Good Practices in Self-supervised Video Representation Learning. *arXiv:2010.15464 [cs]*, April 2021. arXiv: 2010.15464.
- [37] Bruno Degardin and Hugo Proenca. Human Activity Analysis: Iterative Weak/Self-Supervised Learning Frameworks for Detecting Abnormal Events. In *2020 IEEE International Joint Conference on Biometrics (IJCB)*, pages 1–7, Houston, TX, USA, September 2020. IEEE.
- [38] Minseok Seo, Donghyeon Cho, Sangwoo Lee, Jongchan Park, Daehan Kim, Jaemin Lee, Jingi Ju, Hyeoncheol Noh, and Dong-Geol Choi. A Self-Supervised Sampler for Efficient Action Recognition: Real-World Applications in Surveillance Systems. *IEEE Robotics and Automation Letters*, 7(2):1752–1759, April 2022.
- [39] Du Tran, Heng Wang, Lorenzo Torresani, Jamie Ray, Yann LeCun, and Manohar Paluri. A Closer Look at Spatiotemporal Convolutions for Action Recognition. *arXiv:1711.11248 [cs]*, April 2018. arXiv: 1711.11248.
- [40] Du Tran, Lubomir Bourdev, Rob Fergus, Lorenzo Torresani, and Manohar Paluri. Learning Spatiotemporal Features with 3D Convolutional Networks. *arXiv:1412.0767 [cs]*, October 2015. arXiv: 1412.0767.
- [41] Joao Carreira and Andrew Zisserman. Quo Vadis, Action Recognition? A New Model and the Kinetics Dataset. *arXiv:1705.07750 [cs]*, February 2018. arXiv: 1705.07750.
- [42] Zhaofan Qiu, Ting Yao, and Tao Mei. Learning Spatio-Temporal Representation with Pseudo-3D Residual Networks. *arXiv:1711.10305 [cs]*, November 2017. arXiv: 1711.10305.
- [43] Oresti Banos, Juan-Manuel Galvez, Miguel Damas, Hector Pomares, and Ignacio Rojas. Window Size Impact in Human Activity Recognition. *Sensors*, 14(4):6474–6499, April 2014.

- [44] Fredro Harjanto, Zhiyong Wang, Shiyang Lu, Ah Chung Tsoi, and David Dagan Feng. Investigating the impact of frame rate towards robust human action recognition. *Signal Processing*, 124:220–232, July 2016.
- [45] Paulius Micikevicius, Sharan Narang, Jonah Alben, Gregory Diamos, Erich Elsen, David Garcia, Boris Ginsburg, Michael Houston, Oleksii Kuchaiev, Ganesh Venkatesh, and Hao Wu. Mixed Precision Training. *arXiv:1710.03740 [cs, stat]*, February 2018. arXiv: 1710.03740.
- [46] Donglai Wei, Joseph Lim, Andrew Zisserman, and William T Freeman. Learning and Using the Arrow of Time. In *2018 IEEE/CVF Conference on Computer Vision and Pattern Recognition*, pages 8052–8060, Salt Lake City, UT, June 2018. IEEE.
- [47] Li Jing, Pascal Vincent, Yann LeCun, and Yuandong Tian. Understanding Dimensional Collapse in Contrastive Self-supervised Learning. *arXiv:2110.09348 [cs]*, February 2022. arXiv: 2110.09348.
- [48] H. Kuehne, H. Jhuang, E. Garrote, T. Poggio, and T. Serre. HMDB: a large video database for human motion recognition. In *Proceedings of the International Conference on Computer Vision (ICCV)*, 2011.
- [49] Khurram Soomro, Amir Roshan Zamir, and Mubarak Shah. UCF101: A Dataset of 101 Human Actions Classes From Videos in The Wild. *arXiv:1212.0402 [cs]*, December 2012. arXiv: 1212.0402.
- [50] Waqas Sultani, Chen Chen, and Mubarak Shah. Real-world Anomaly Detection in Surveillance Videos. *arXiv:1801.04264 [cs]*, February 2019. arXiv: 1801.04264 version: 3.
- [51] Kensho Hara, Hirokatsu Kataoka, and Yutaka Satoh. Can Spatiotemporal 3D CNNs Retrace the History of 2D CNNs and ImageNet? In *2018 IEEE/CVF Conference on Computer Vision and Pattern Recognition*, pages 6546–6555, Salt Lake City, UT, USA, June 2018. IEEE.